Contributions to membrane-embedded-protein diffusion beyond hydrodynamic theories

Brian A. Camley and Frank L. H. Brown

Phys. Rev. E **85**, 061921 — Published 25 June 2012

DOI: 10.1103/PhysRevE.85.061921

Contributions to membrane-embedded-protein diffusion beyond hydrodynamic theories

Brian A. Camley[1] and Frank L. H. Brown[2,1]

[1]*Department of Physics, University of California, Santa Barbara, California 93106, USA*
[2]*Department of Chemistry and Biochemistry, University of California, Santa Barbara, California 93106, USA*

The diffusion coefficients of proteins embedded in a lipid membrane are traditionally described by the hydrodynamic Saffman-Delbrück theory, which predicts a weak dependence of the diffusion coefficient on protein radius, $D \sim \ln R$. Recent experiments have observed a stronger dependence, $D \sim 1/R$. This has led to speculation that the primary sources of drag on the protein are not hydrodynamic, but originate in coupling to other fields, such as lipid chain stretching or tilt. We discuss a generic model of a protein coupled to a nonconserved scalar order parameter (e.g. chain stretching), and show that earlier results may not be as universal as previously believed. In particular, we note that the drag depends on the way the protein-order parameter coupling is imposed. In this model, $D \sim 1/R$ can be obtained if the protein is much larger than the order parameter correlation length. However, if we modify the model to include advection of the order parameter, which is a more appropriate assumption for a fluid membrane, we find that the entrainment of the order parameter by the protein's motion significantly changes the scaling of the diffusion coefficient. For parameters appropriate to protein diffusion, the Saffman-Delbrück-like scaling is restored, but with an effective radius for the protein that depends on the order parameter's correlation length. This qualitative difference suggests that hydrodynamic effects cannot be neglected in the computation of drag on a protein interacting with the membrane.

PACS numbers: 87.16.dp,87.16.dj,47.63.mf,87.15.kt

Lipid bilayer membranes are a fundamental component of biological cells, and play a role in many essential biological processes, including compartmentalization of the cell and organelles, as well as cell signaling, in which the membrane is the environment for the relevant membrane proteins [1]. Interactions between the membrane and embedded proteins may alter the functioning of the proteins [2] as well as potentially leading to protein aggregation [3]. The diffusion coefficient of proteins in the membrane has traditionally been described by the Saffman-Delbrück law [4–6], which predicts that the diffusion coefficient of a protein should depend only logarithmically on the protein radius, $D \sim \ln(R)$. This prediction has be used to determine the size of membrane-embedded objects and protein aggregates [7, 8]. However, recent experiments have measured protein diffusion coefficients that have a stronger dependence on protein radius, $D \sim 1/R$ [9–11], though this is not universally accepted [12, 13]. Naji, Levine, and Pincus (NLP) suggested that this dependence could arise from dissipative protein-lipid interactions, such as a coupling to local lipid conformation (e.g. chain stretching or tilt) [14] (Fig. 1). Démery and Dean (DD) have described an interesting class of these "coupling models," and shown that the case of a linear coupling to a field with simple relaxational dynamics can be solved exactly [15, 16]. The dynamics of proteins with hydrophobic mismatch (i.e. a coupling to membrane thickness) has also been treated by coarse-grained molecular dynamics simulations [13, 17], and the dynamics of proteins with a preferred spontaneous curvature calculated with continuum approaches [18, 19].

We extend the approach of Démery and Dean [15, 16], treating a model of a protein coupled to a nonconserved "Model A" order parameter $\phi(\mathbf{r}, t)$ [20, 21]. We apply this coupling as a boundary condition, and show that this model can be solved exactly to determine the additional drag from the protein-lipid interaction. We then discuss some distinctions between this model and the model originally suggested by DD, which has identical Model A dynamics for the field, but a linear protein-field coupling. We suggest that coupling the external field to the protein via a boundary condition may be more appropriate for describing the protein-lipid interaction. We then extend the model to describe the coupling with a nonconserved order parameter that is hydrodynamically advected ("Advected Model A"); the order parameter is then entrained by the protein, which significantly alters the magnitude and scaling properties of the diffusion coefficient. This set of assumptions is more appropriate for a fluid membrane, as it allows the membrane to flow in response to protein motion.

Our goal in all portions of this paper will be to determine the drag force on a protein moving with a fixed velocity through an order parameter field $\phi(\mathbf{r}, t)$. In Section I of the paper, we will follow [15, 16] and assume that the order parameter field is not advected by the lipid flow around the protein, and that the lipid flow is not altered by the inhomogeneity of the order parameter. In that case, we find the drag force due solely to the order-parameter interaction, $\mathbf{F}^{\text{int}}_{\text{drag}} = -\zeta_I \mathbf{V}_p$ where $\mathbf{V}_p$ is the particle velocity. The total drag will then be $\zeta_{\text{tot}} = \zeta_I + \zeta_{\text{hydro}}$, where by assumption the hydrodynamic drag ζ_{hydro} is just the usual Saffman-Delbrück drag [4], and the diffusion coefficient $D = k_B T/\zeta_{\text{tot}}$ by the Stokes-Einstein relation [21, 22]. In Section II, we explicitly include the advection of the order parameter by the lipid flow around the protein, and determine the total drag by integrating the stress tensor around the protein.

We do not give the order parameter $\phi(\mathbf{r}, t)$ a direct physical interpretation, but note that the Model A dynamics are the simplest possible phenomenological model of a nonconserved scalar lipid feature, such as lipid conformation [2, 23–25]. The combination of the advection-diffusion and hydrodynamic equations we present here are a very simplified version of those used to model liquid crystals [26–28]. Extensions of this research to coupling to more complex lipid

characteristics (e.g. tilt and thickness [29]), may be possible, though the dynamics of these fields are still not completely understood [30–32].

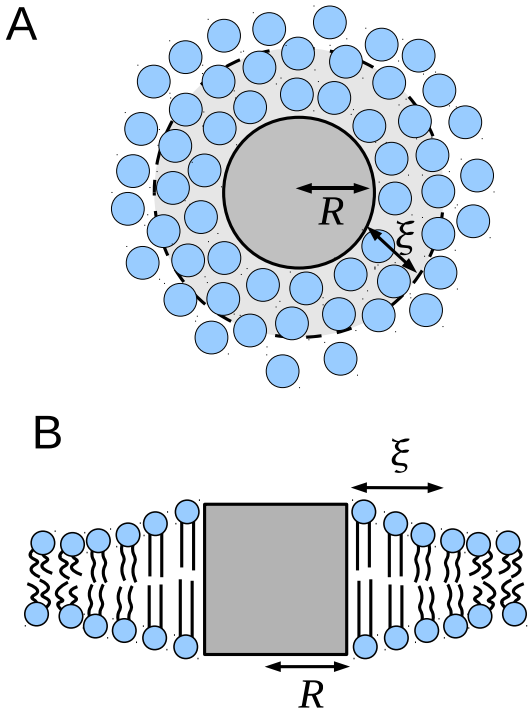

FIG. 1. (Color online). A: Schematic illustration of a protein-induced distortion in a lipid membrane from top of membrane. Lipids within a distance of roughly ξ of the protein may have altered properties, such as chain conformation. B: One particular example of distortion, in which hydrophobic mismatch leads to a change in membrane thickness.

I. MODEL A DYNAMICS

Démery and Dean [15, 16] have suggested applying a simple dissipative model to describe the dynamics of a nonconserved order parameter in a membrane. This model, which we refer to as "Model A" dynamics (in the classification of Hohenberg and Halperin [20]), describes the relaxation of the order parameter to its equilibrium value with a phenomenological relaxation time τ. Although scalar order parameters with similar energetics have previously been used to describe chain order in membranes (see, e.g. [24, 25, 33]), we do not give a specific physical interpretation for the field ϕ, as we do not have a good reason to believe that Model A is a realistic physical model for the relaxation of any of these order parameters. The primary reason for working with Model A is that it is the simplest possible dynamical model for a nonconserved order parameter. Similar models have also been proposed phenomenologically for the relaxation of the nematic order parameter [34, 35], though to reach the simple one-relaxation-time approximation of Eq. 2 requires neglecting fluid flow.

We discuss this model to show in a simple context that the drag on the protein depends on the way the coupling between the protein and the order-parameter is treated, i.e. as a boundary condition, as in most of this paper, or a linear interaction, as in [15, 16]. This section also serves as an introduction to the more complicated and realistic model of Section II, where we will show explicitly that hydrodynamic effects cannot be neglected.

Model A describes a scalar field $\phi(\mathbf{r},t)$ with a Hamiltonian

$$H = \mathcal{E}\int d^2r\left[\frac{1}{2}\phi^2(\mathbf{r}) + \frac{\xi^2}{2}|\nabla\phi|^2\right] \tag{1}$$

where $\mathcal{E}$ is an energy density and ξ the correlation length of the field. The dynamics of this field are then given by

$$\partial_t\phi(\mathbf{r},t) = -\Gamma\frac{\delta H}{\delta\phi(\mathbf{r},t)} + \nu(\mathbf{r},t) \tag{2}$$

$$= -\Gamma\mathcal{E}\left(\phi - \xi^2\nabla^2\phi\right) + \nu(\mathbf{r},t) \tag{3}$$

where Γ is a phenomenological transport coefficient, with $1/\Gamma\mathcal{E} \equiv \tau$ the relaxation time of the system. $\nu(\mathbf{r},t)$ is a Gaussian Langevin force with variance $\langle\nu(\mathbf{r},t)\nu(\mathbf{r}',t')\rangle = 2k_BT\,\Gamma\delta(\mathbf{r}-\mathbf{r}')\delta(t-t')$, as required by the fluctuation-dissipation theorem [21]. For the remainder of the paper, we will neglect the fluctuations; this point will be discussed in Section III.

A. Model A with boundary condition

We determine the drag on a protein moving with a fixed velocity $\mathbf{V}_p$. The protein influences the order parameter around it, which we represent by fixing the field ϕ to the value ϕ_b on the protein surface. Near the protein, ϕ will then take on a value different from equilibrium value of $\phi = 0$ (Fig. 2).

If we change frames to the reference frame of the particle, the equation of motion Eq. 2 becomes (at steady state, and neglecting fluctuations)

$$-\mathbf{V}_p\cdot\nabla\phi = -\frac{1}{\tau}\left(\phi - \xi^2\nabla^2\phi\right) \tag{4}$$

where $\tau = 1/\Gamma\mathcal{E}$ is the field's relaxation time. We emphasize here that $\mathbf{V}_p$ is simply the protein's velocity, and in this model we have not explicitly considered the advection of the order parameter; this assumption will be examined in Section II. We determine the field $\phi(\mathbf{r},t)$ perturbatively in the protein velocity $\mathbf{V}_p$ [36]. We take $\mathbf{V}_p = V_0\hat{\mathbf{x}}$ without loss of generality, and expand $\phi(\mathbf{r},t) \approx \phi_{(0)}(\mathbf{r}) + V_0\,\phi_{(1)}(\mathbf{r},t)$. To zeroth order in V_0, ϕ must be time-independent and radially symmetric. The boundary condition on ϕ is that $\phi(r=R) = \phi_b$, where R is the protein radius (see Fig. 2), and $\phi(r) \to 0$ as $r\to\infty$. With these boundary conditions, we solve Eq. 4 to zeroth order in V_0 to find

$$\phi_{(0)}(\mathbf{r}) = \phi_b\frac{K_0(r/\xi)}{K_0(R/\xi)} \tag{5}$$

where $K_n(x)$ is the n^{th}-order modified Bessel function of the second kind. We note that $\phi(\mathbf{r},t)$ is only defined for $r \geq R$.

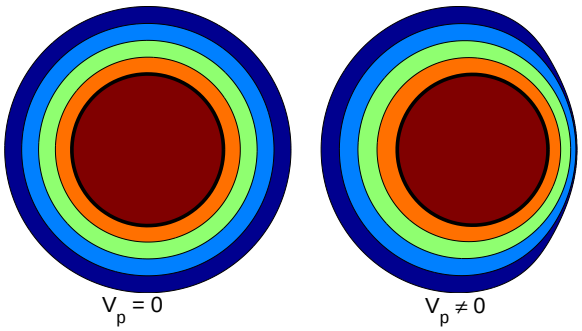

FIG. 2. (Color online). Illustration of the $\phi(\mathbf{r},t)$ profile. For the static protein (left), $\phi(\mathbf{r},t)=\phi_{(0)}(r)$ is given by Eq. 5. For a protein moving at constant rightward velocity (right), $\phi(\mathbf{r},t)=\phi_{(0)}(r)+V_0\phi_{(1)}(r,\theta)$. The contours shown are logarithmically spaced, i.e. $\phi=\phi_b$ at the thick contour ($r=R$), and $\phi=0.1\phi_b$ at the next contour out.

To determine the drag force, we have to integrate the stress tensor for the field around the inclusion. The stress tensor Π_{ij} for the ϕ field can be derived by looking at small deformations of the system, and determining the change in the energy H [37, 38]. The result is [37–39]

$$\Pi_{ij}(\mathbf{r})/\mathcal{E}=\delta_{ij}\left[\frac{1}{2}\phi^2+\frac{\xi^2}{2}|\nabla\phi|^2\right]-\xi^2(\nabla_i\phi)(\nabla_j\phi) \quad (6)$$

i.e. $\nabla\cdot\Pi=\frac{\delta H}{\delta\phi}\nabla\phi$. The total force, which is in the $\hat{\mathbf{x}}$ direction by symmetry, is $\mathbf{F}^{\rm int}_{\rm drag}=\oint d\ell\,\Pi\cdot\hat{\mathbf{n}}=F\hat{\mathbf{x}}$,

$$F=R\int_0^{2\pi}d\theta\;\Pi_{xj}(r=R,\theta)\hat{n}_j \quad (7)$$

where $\hat{n}_j$ is the outward-pointing normal to the circle and the Einstein summation convention is assumed. In principle, we would need to determine $\phi(\mathbf{r})$ to first order in V_0 to determine F, as the force is $O(V_0)$; we do this calculation in Appendix A. However, we can avoid explicitly calculating $\phi_{(1)}$ by using the steady-state equation Eq. 4, letting us set $\nabla\cdot\Pi=\frac{\delta H}{\delta\phi}\nabla\phi=\Gamma^{-1}\,(\mathbf{V}_p\cdot\nabla\phi)\,\nabla\phi$. Thus, to first order, $\nabla\cdot\Pi$ will only depend on $\phi_{(0)}$. By applying the divergence theorem to Eq. 7,

$$\mathbf{F}^{\rm int}_{\rm drag}=-\int_{r\geq R}d^2r\,\nabla\cdot\Pi \quad (8)$$

$$\approx-\frac{1}{\Gamma}\int_{r\geq R}d^2r\,\mathbf{V}_p\cdot\nabla\phi_{(0)}\nabla\phi_{(0)} \quad (9)$$

where the second line is correct to first order in V_0. We could equivalently have determined this equation by considering the power dissipated (as in [18]), $P=\frac{dH}{dt}=\int d^2r\frac{\delta H}{\delta\phi(\mathbf{r})}\frac{d\phi(\mathbf{r})}{dt}=-\frac{1}{\Gamma}\int d^2r(\mathbf{V}_p\cdot\nabla\phi)^2=\mathbf{F}^{\rm int}_{\rm drag}\cdot\mathbf{V}_p$.

Eq. 9 can be integrated straightforwardly, and we find $\mathbf{F}^{\rm int}_{\rm drag}=-\zeta_I\mathbf{V}_p$, with

$$\zeta_I=\zeta_c\beta\left[\frac{\beta K_0(\beta)^2+2K_0(\beta)K_1(\beta)-\beta K_1(\beta)^2}{2K_0(\beta)^2}\right] \quad (10)$$

where $\beta=R/\xi$ is the ratio of the protein radius to the interface width, which is the relevant unitless measure of the protein size; $\zeta_c=\pi\phi_b^2/\Gamma$ is the characteristic scale of the drag. The interaction drag ζ_I has the asymptotic behavior

$$\zeta_I/\zeta_c\sim\begin{cases}-\frac{1/2+\gamma_E+\ln(\beta/2)}{[\gamma_E+\ln(\beta/2)]^2} & \beta\ll1\\ \beta/2 & \beta\gg1\end{cases} \quad (11)$$

where $\gamma_E\approx0.5772\ldots$ is the Euler-Mascheroni constant. These asymptotic results and the exact result are plotted in Fig. 3.

We see that we recover the $\zeta_I\sim R$ scaling in the limit $R\gg\xi$, as predicted by NLP's scaling arguments. We also observe that ζ_I has a weak (logarithmic) dependence on R for $R\ll\xi$.

While the large R dependence of ζ_I on R is clearly predicted by the scaling arguments of NLP, the dependence on ξ ($\zeta_I\sim1/\xi$) is less obvious. However, it is a consequence of dimensional analysis along with NLP's prediction $\zeta_I\sim R$. The only independent parameters in our model are R, ξ, Γ, τ, and ϕ_b; constructing a variable with the units of drag shows us that $\zeta_I=\Gamma^{-1}f(R/\xi,\phi_b)$, as we see in Eq. 10. Thus, as ζ_I can only depend on R and ξ through $\beta=R/\xi$, $\zeta_I\sim R$ implies $\zeta_I\sim1/\xi$. In other words, as the interface width ξ is decreased, the drag ζ_I *increases*. This singular behavior is a remnant of the unphysical assumption that the lipids' velocity is uncorrelated with the protein velocity; in a fluid membrane, the increasing stress near the protein will lead to lipid flow, as we will see in Section II, which will change this behavior.

When will the order parameter-induced drag be the primary source of drag? Our initial assumption in this section is that the presence of order parameter inhomogeneities does not affect the lipid flow around the protein, or the hydrodynamic drag; this assumption is obviously suspect, and we will address it in Section II. However, with this assumption, the total drag on the protein is $\zeta_{\rm tot}=\zeta_I+\zeta_{\rm hydro}$, with $\zeta_{\rm hydro}$ given by the Saffman-Delbrück drag [4, 5, 40], if the protein is in a free membrane, or by the Evans-Sackmann [41] or Stone-Ajdari [42] theories for proteins in supported membranes. For proteins, $\zeta_{\rm hydro}\sim\eta_m$, where η_m is the membrane's surface viscosity [4]. If ζ_I is given by Eq. 10, then for a fixed radius R, the interaction drag will be much larger than the hydrodynamic drag if $\chi\gg1$, where $\chi\equiv\phi_b^2/\eta_m\Gamma$. In Section II, we will see that χ is still a relevant parameter when advection is included, and that the order parameter drag can be neglected if $\chi\ll1$; however, $\chi\gg1$ is not sufficient to make hydrodynamics irrelevant.

B. Model A with linear interaction: comparison with Démery and Dean result

Démery and Dean also study Model A dynamics (as well as other dissipative models), but couple the protein to the field with a linear interaction, rather than a boundary condition. We show that their model as formulated in [15, 16] results in a different drag than the boundary-condition model, but that their result is sensitive to the method used to choose the strength of

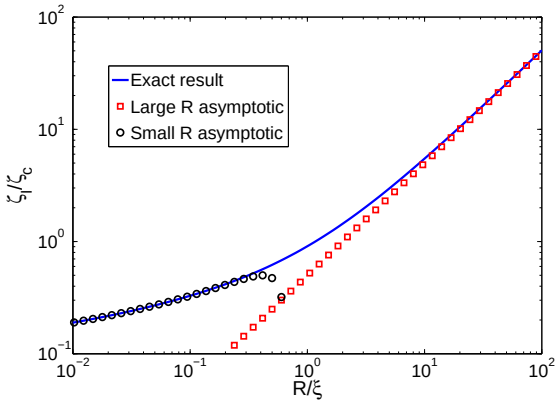

FIG. 3. (Color online). The drag from interaction with the external field (Eq. 10) in the boundary condition model scales linearly with protein size for proteins with a radius much larger than the field's correlation length ($R \gg \xi$). However, in the limit $R \ll \xi$, $\zeta_I \sim 1/\ln(R)$ (Eq. 11).

the linear protein-field interaction. If we make a different prescription for this interaction, the DD results match with our approach in Section I A.

The DD model considers a membrane inclusion with position $\mathbf{R}_p(t) = \mathbf{V}_p t$ interacting with a classical field $\phi(\mathbf{r}, t)$ with a Gaussian Hamiltonian $H = H_0 + H_{\rm int}(t)$,

$$H_0 = \frac{1}{2}\int d^d r \phi(\mathbf{r})\Delta\phi(\mathbf{r}) \tag{12}$$

$$H_{\rm int}(t) = h\int d^d r \phi(\mathbf{r}) K(\mathbf{r} - \mathbf{R}_p(t)) \tag{13}$$

where Δ is a positive self-adjoint operator and $K(\mathbf{r})$ is an "envelope" function localized near $\mathbf{r} = 0$ and with the characteristic size R, e.g. $K(\mathbf{r}) = \frac{1}{2\pi R^2} e^{-r^2/2R^2}$. For simplicity of calculation, DD treat $K(\mathbf{r})$ as applying a cutoff in momentum space, $K_{\mathbf{k}} = \theta(\pi/R - k)$ for the Model A coupling, where θ is the Heaviside function. The Fourier transform conventions used here are $f_{\mathbf{k}} = \int d^2 r e^{-i\mathbf{k}\cdot\mathbf{r}} f(\mathbf{r})$, $f(\mathbf{r}) = \int \frac{d^2k}{(2\pi)^2} e^{i\mathbf{k}\cdot\mathbf{r}} f_{\mathbf{k}}$.

The class of dissipative models studied by DD is

$$\partial_t \phi = -\Gamma \frac{\delta H}{\delta\phi(\mathbf{r})} + \nu(\mathbf{r}, t) \tag{14}$$

where Γ is a positive self-adjoint operator and ν is a Langevin force obeying the fluctuation-dissipation relation.

In two dimensions, Démery and Dean find $\mathbf{F}^{\rm int}_{\rm drag} = -\frac{\partial H_{\rm int}}{\partial \mathbf{R}_p} = -\zeta_I^{\rm DD}\mathbf{V}_p$, with

$$\zeta_I^{\rm DD} = h^2 \int \frac{d^2k}{(2\pi)^2} \frac{k_x^2 |K_{\mathbf{k}}|^2}{\Delta_{\mathbf{k}}^2 \Gamma_{\mathbf{k}}} \tag{15}$$

where for Model A, $\Delta_{\mathbf{k}} = \mathcal{E}(1 + k^2\xi^2)$ and $\Gamma_{\mathbf{k}} = \Gamma$ (see Eqs. 1-2).

DD set h by requiring that the static insertion energy, $E_{\rm ins} = -\frac{h^2}{4\pi}\int_0^\infty dk k |K_{\mathbf{k}}|^2/\Delta_{\mathbf{k}}$ scale as a line energy, $E_{\rm ins} = -2\pi\gamma_I R$. With the choice $K_{\mathbf{k}} = \theta(\pi/R - k)$, we find that $h^2 = 16\pi^2\gamma_I \mathcal{E} R\xi^2/\ln(1 + \pi\xi^2/R^2)$. Evaluating ζ_I from Eq. 15, we find

$$\zeta_I^{\rm DD} = \zeta_c^{\rm DD}\beta\left[1 - \frac{\pi^2}{(\pi^2 + \beta^2)\ln(1 + \pi^2/\beta^2)}\right] \tag{16}$$

where $\beta = R/\xi$ and $\zeta_c^{\rm DD} = \frac{2\pi\gamma_I}{\Gamma\xi\mathcal{E}}$ is the characteristic scale of the drag in the DD model. For small and large proteins, this result takes on the asymptotic forms,

$$\zeta_I^{\rm DD}/\zeta_c^{\rm DD} \sim \begin{cases} \beta\frac{1 + 2\log\beta/\pi}{2\log\beta/\pi} & \beta \ll 1 \\ \frac{\pi^2}{2}\frac{1}{\beta} & \beta \gg 1 \end{cases} \tag{17}$$

The DD model predicts that the drag coefficient will increase with protein radius R only if $R \ll \xi$, where ξ is the correlation length. DD do not consider the limit of $R \gg \xi$ explicitly, but if we assume that the form $K_{\mathbf{k}} = \theta(\pi/R - k)$ is still appropriate, the DD model predicts that the drag coefficient will actually *decrease* as $1/R$. This should be contrasted with the behavior determined from the boundary-condition coupling (Eq. 11), which crosses over from logarithmic behavior for $R \ll \xi$ to $\zeta_I \sim R$ as $R \gg \xi$. We argue that our model is more consistent with the scaling analysis of [14], which requires $R \gg \xi$ as a necessary condition to guarantee that $\zeta_I \sim R$.

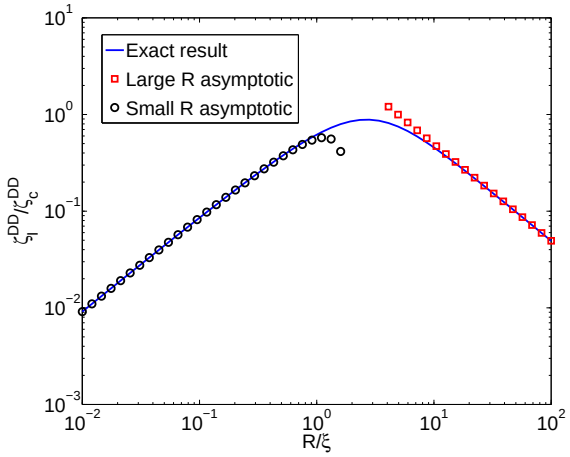

FIG. 4. (Color online). The DD model [16], Eq. 16 predicts a drag coefficient $\zeta_I^{\rm DD}$ that scales linearly in protein size for $R \ll \xi$, but if we extend it naively into the limit $R \gg \xi$, $\zeta_I^{\rm DD}$ decreases with increasing protein size (Eq. 17).

The inconsistency between the results of DD and the results of Section I A and the scaling analysis of NLP [14] results from the different handling of the protein-field interaction (boundary condition for Section I A or linear coupling for DD). However, by exploiting the freedom to choose the envelope function $K(\mathbf{r})$ and the interaction scale h, we can make the DD model consistent with the boundary-condition model.

We first note that Eq. 15 can be rewritten as

$$\zeta_I^{\rm DD} = \int \frac{d^2k}{(2\pi)^2}\frac{k_x^2}{\Gamma_{\mathbf{k}}}\left|\phi_{(0)}^{\rm DD}(\mathbf{k})\right|^2 \tag{18}$$

$$= \frac{1}{\Gamma}\int d^2r\left|\hat{\mathbf{x}}\cdot\nabla\phi_{(0)}^{\rm DD}(\mathbf{r})\right|^2 \text{ (Model A)} \tag{19}$$

where $\phi_{(0)}^{\rm DD}$ is the static profile for the DD model, $\phi_{(0)}^{\rm DD}(\mathbf{k}) = -hK_{\mathbf{k}}/\Delta_{\mathbf{k}}$. $\phi_{(0)}^{\rm DD}$ is the steady-state solution to Eq. 14, i.e. it minimizes $H_0 + H_{\rm int}$. Eq. 19 holds only for the specific case of Model A, when $\Gamma_{\mathbf{k}} = \Gamma$. By comparison to Eq. 9, the DD approach and the boundary-condition model will give identical results if $\phi_{(0)}^{\rm DD}(\mathbf{r}) = \phi_{(0)}(\mathbf{r})$, where $\phi_{(0)}$ is the equilibrium field from the boundary condition model (Eq. 5). This means that if the envelope function $K(\mathbf{r})$ is chosen so that the distortion around the protein matches that of the boundary-condition model of Section I A, the drag will be identical to that of the boundary-condition model (Eq. 10). We can also ensure that $\zeta_I = \zeta_I^{\rm DD}$ without changing the envelope function by changing the prescription for h, e.g. by choosing h such that

$$\int_{\mathbb{R}^2} d^2r\left|\hat{\mathbf{x}}\cdot\nabla\phi_{(0)}^{\rm DD}(\mathbf{r})\right|^2 = \int_{r\geq R} d^2r\left|\hat{\mathbf{x}}\cdot\nabla\phi_{(0)}(\mathbf{r})\right|^2 \tag{20}$$

One could certainly be skeptical about the process of assigning h to be a complicated function of R; after all, as is clear from Eq. 15, the choice of h can completely determine $\zeta_I^{\rm DD}$. We note that it is also possible to get scaling consistent with Section I A ($\zeta_I \sim 1/\ln\beta$ for $\beta \ll 1$) by weaker assumptions. One possible way is using the cutoff function $K_{\mathbf{k}} = \theta(\pi/R - k)$, and then choosing h to ensure that the boundary condition $\phi_{(0)}^{\rm DD}(r=R) = \frac{-h}{2\pi\mathcal{E}\xi^2}\int_0^{\pi/\beta} du\, J_0(u\beta)\frac{u}{1+u^2} = \phi_b$ holds. In this case,

$$\zeta_I^{\rm DD}/\zeta_c = \frac{1}{2}\frac{\ln\left[1+\frac{\pi^2}{\beta^2}\right] - \frac{\pi^2}{\pi^2+\beta^2}}{\left(\int_0^{\pi/\beta} du\, J_0(u\beta)\frac{u}{1+u^2}\right)^2} \tag{21}$$

where, as in Section I A, $\zeta_c = \pi\phi_b^2/\Gamma$. Numerically evaluating Eq. 21 shows that $\zeta_I^{\rm DD}/\zeta_c \approx -1.0097/\ln(\beta)$ for $\beta \ll 1$ (with maximum relative error 3×10^{-3} for β from 10^{-12} to 10^{-6}), consistent with the scaling of Eq. 10 for $\beta \ll 1$.

We also argue that the procedure for determining h used in [16] may not be appropriate for other reasons. We note that the suggested requirement $E_{\rm ins} \sim R$ is not reasonable for all values of R/ξ. Throughout [16], DD assume that $R \ll \xi$ (the deformation is much larger than the protein); if this is the case, the deformed area surrounding the protein will be roughly $\pi\xi^2 - \pi R^2 \approx \pi\xi^2$, and we would expect only a weak dependence of the insertion energy on the protein size. More explicitly, within the boundary condition model of Section I A, the insertion energy will be given by $E_{\rm ins} \equiv H[\phi_{(0)}] = \pi\mathcal{E}\phi_b^2\xi^2\beta K_1(\beta)/K_0(\beta)$, with $\beta = R/\xi$. For $R \ll \xi$ we find that $E_{\rm ins} \approx -\pi\mathcal{E}\xi^2\phi_b^2\left[\gamma_E + \ln(\beta/2)\right]^{-1}$, showing a weak dependence on R, as suggested by our rough estimate.

II. EFFECTS OF HYDRODYNAMIC ADVECTION OF ORDER PARAMETER (ADVECTED MODEL A)

Both our model of Section I A and that of DD assume that the order parameter ϕ is not advected by fluid flow, i.e. that lipids are at rest, even near the translating protein (Fig. 5). This assumption is apparent in Eq. 4. In addition, the models of Section I do not allow the material to flow in response to the applied stress Π; they describe a solid. These assumptions are not generally appropriate for lipid membranes in their fluid phase, which are well-described by hydrodynamic theories [4, 43]. In particular, molecular dynamics simulations show that lipids near a diffusing protein are entrained by the protein, and have velocities correlated to the protein motion [44]. If some lipids within ξ of the protein move in concert with the protein, the distortion of $\phi(\mathbf{r},t)$ due to protein motion and therefore the drag ζ_I will be significantly reduced (Fig. 5, right). The hydrodynamic flow caused by the stress Π will also lead to an alteration of the drag on the protein due to hydrodynamic dissipation.

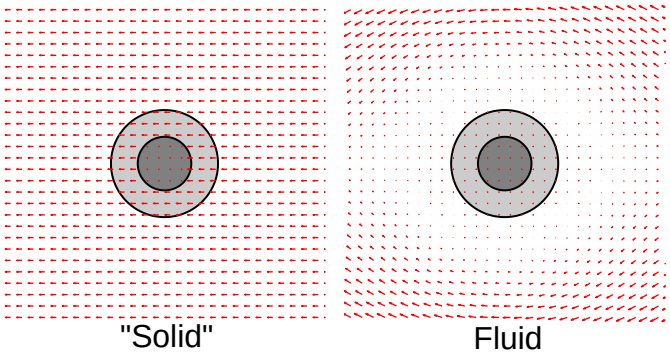

FIG. 5. (Color online). Lipid velocities plotted in the frame moving with the protein. The dark central circle is the protein, and the lighter circle the region with $\phi(\mathbf{r})$ significantly different from 0. The models of Section I make the assumption that the lipids are at rest relative to the protein, i.e. that they have velocity $-\mathbf{V}_p$ in the protein's rest frame; this is illustrated in the left panel. In a fluid membrane, the lipid velocity will be entrained by the protein motion (right). The distortion of the profile $\phi(\mathbf{r})$ will be significantly reduced in this case, compared to that of Section I.

If ϕ is advected by a velocity field in the membrane $\mathbf{v}_m$, we describe the dynamics of the field ϕ, in the protein's reference frame as (in steady state)

$$(\mathbf{v}_m - \mathbf{V}_p)\cdot\nabla\phi(\mathbf{r}) = -\Gamma\frac{\delta H}{\delta\phi} \tag{22}$$

$$= -\frac{1}{\tau}\left(\phi - \xi^2\nabla^2\phi\right) \tag{23}$$

where now $\mathbf{v}_m$ is the membrane velocity measured in the lab frame, i.e. $\mathbf{v}_m = \mathbf{V}_p$ at $r = R$, and $\mathbf{v}_m \to 0$ as $r \to \infty$. We will work in polar coordinates $\mathbf{v}_m(r,\theta) = v_m^r\hat{\mathbf{r}} + v_m^\theta\hat{\theta}$. This advection-diffusion model, which we call "Advected Model A", is the simplest possible model to represent the dynamics of a nonconserved order parameter in a *fluid* lipid bilayer membrane.

The total drag force on the protein is (see, e.g. [27, 45] for similar calculations)

$$\mathbf{F}_{\text{drag}} = \oint d\ell\, (\sigma + \Pi) \cdot \hat{\mathbf{n}} \tag{24}$$

where the integral is around the boundary of the protein, $\hat{\mathbf{n}}$ is the outward-pointing normal, Π is the composition stress tensor (Eq. 6) and σ the hydrodynamic stress tensor,

$$\sigma_{ij} = -P\delta_{ij} + \eta_m \left(\frac{\partial v_m^i}{\partial r_j} + \frac{\partial v_m^j}{\partial r_i} \right) \tag{25}$$

where P is the membrane surface pressure and η_m the membrane surface viscosity. In Section I, we only calculated one piece of $\mathbf{F}_{\text{drag}}$, $\mathbf{F}_{\text{drag}}^{\text{int}} = \oint d\ell\, \Pi \cdot \hat{\mathbf{n}}$ (Eq. 7). Our approach in this section will be to calculate $\mathbf{F}_{\text{drag}}$ from Eq. 24, and then determine ζ_{tot}, i.e.

$$\mathbf{F}_{\text{drag}}^{\text{total}} = -\zeta_{\text{tot}} \mathbf{V}_p \tag{26}$$

We have, in Eq. 26, included the possibility of there being additional sources of drag beyond that in Eq. 24, i.e. $\mathbf{F}_{\text{drag}}^{\text{total}} = \mathbf{F}_{\text{drag}} + \mathbf{F}_{\text{additional}}$ with $\mathbf{F}_{\text{drag}}$ from Eq. 24. The "intrinsic drag" that Evans and Sackmann include [41] is of this form, and we will treat this term below; we also will include an appropriate intrinsic drag of this sort in our calculations of ζ_{tot}.

To determine $\mathbf{v}_m$ and P, we have to solve the Stokes equations appropriate for a membrane taking into account the body force $\nabla \cdot \Pi = \frac{\delta H}{\delta \phi} \nabla \phi$ exerted by the field on the fluid. Within the Saffman-Delbrück picture of a membrane as a two-dimensional fluid surrounded by a bulk three-dimensional fluid, the membrane Stokes equations are [4, 5, 43, 46–48]

$$\eta_m \nabla^2 \mathbf{v}_m - \nabla P + \mathbb{K} * \mathbf{v}_m + \nabla \cdot \Pi = 0 \tag{27}$$

$$\nabla \cdot \mathbf{v}_m = 0 \tag{28}$$

where $(\mathbb{K} * \mathbf{v}_m)(\mathbf{r}) = \int d^2 r'\, \mathbb{K}(\mathbf{r} - \mathbf{r}') \mathbf{v}_m(\mathbf{r}')$ is the the traction from the outside fluid and the boundary conditions are $\mathbf{v}_m = \mathbf{V}_p$ on $r = R$ and $\mathbf{v}_m \to 0$ as $r \to \infty$. In a free-floating membrane surrounded on both sides by a fluid with viscosity η_f, the Fourier transform of the convolution term is given by $\{\mathbb{K} * \mathbf{v}_m\}_{\mathbf{q}} = -2\eta_f q\, \mathbf{v}_m(\mathbf{q})$, i.e. $\mathbb{K}(\mathbf{q}) = -2\eta_f q$. This nonlocal term makes solving the mobility problem difficult [5]. We will treat the similar case of a membrane above a solid substrate (Fig. 6), which in some limits reduces to a significantly simpler problem. The kernel $\mathbb{K}(\mathbf{q})$ then takes the form [46, 49]

$$\mathbb{K}(\mathbf{q}) = -\eta_f q \coth(qH) - \eta_f q \tag{29}$$

For wavelengths long compared to H ($q \ll 1/H$), this reduces to the form $\mathbb{K}(\mathbf{q}) = -\eta_f/H$, i.e. a linear drag, $\mathbb{K} * \mathbf{v}_m = -\frac{\eta_f}{H} \mathbf{v}_m$ [41, 42]. In fact, this approximation may be appropriate as long as H is small compared to the Saffman-Delbrück length scale $L_{sd} = \eta_m / 2\eta_f$ [42]. This "Brinkman equation" model can also be derived from treating the thin layer of fluid between the membrane and the solid substrate in the lubrication approximation [42]. Though strictly speaking this approximation describes a supported membrane, we expect the hydrodynamics to be in qualitative agreement with that of a free membrane for objects of size $R \ll L_H$, where $L_H^2 \equiv 2L_{sd}H$; see [50, 51] and references therein. For example, we note that the hydrodynamic drag in this theory will have the same functional form as the Saffman-Delbrück law [4] in the limit of $R \ll L_H$, but with L_H instead of L_{sd} the relevant length scale.

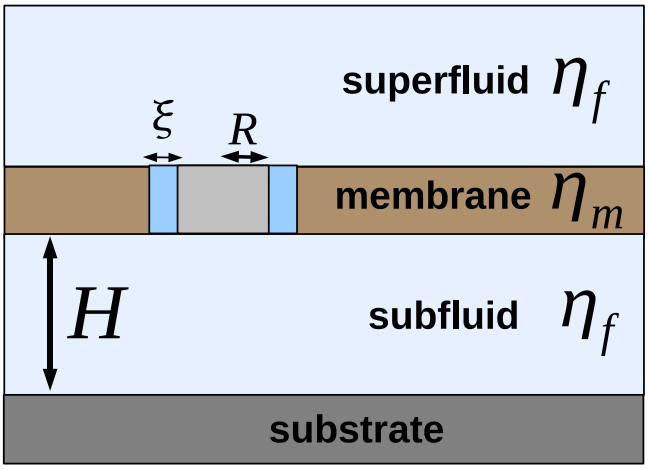

FIG. 6. (Color online). Illustration of protein of radius R diffusing in membrane a height H above a substrate, surrounded by fluid with viscosity η_f. We have also indicated the distorted region near the membrane, with characteristic size ξ.

In the absence of coupling between the protein and the order parameter (i.e. $\phi_b = 0$), the bare hydrodynamic drag is [41]

$$\zeta_{\text{Evans-Sackmann}} = \pi \eta_m \epsilon \left[2\epsilon + \frac{4K_1(\epsilon)}{K_0(\epsilon)} \right] \tag{30}$$

where $\epsilon \equiv R/L_H$. We emphasize that Eq. 30 includes the effect of the intrinsic drag with the substrate, which adds a drag force of $\mathbf{F}_{\text{additional}} = -\pi R^2 b_p \mathbf{V}_p$ [41], where b_p is a phenomenological drag coefficient. We have included this term in Eq. 30, setting $b_p = \eta_f / H$, which is appropriate for a membrane separated by a thin layer of fluid from a substrate. This term accounts for the drag on the bottom of the protein; see [41, 42] for details. We also include this term in our numerical calculations of ζ_{tot} for Advected Model A, so that ζ_{tot} is equal to Eq. 30 when the coupling to the order parameter vanishes ($\phi_b = 0$).

In principle, the advection equation (Eq. 22) and the membrane Stokes equations (Eqs. 27-28) must be solved simultaneously in order to determine $\mathbf{v}_m$, $\phi(\mathbf{r})$ and P. However, we can again exploit the simplicity of the order parameter dynamics and use Eq. 22 to calculate the force $\mathbf{f}_\phi = \frac{\delta H}{\delta \phi} \nabla \phi = -\frac{1}{\Gamma} (\mathbf{v}_m - \mathbf{V}_p) \cdot \nabla \phi \nabla \phi$. To linear order in V_0, this force only depends on the static profile $\phi_{(0)}$, and we can eliminate Eq. 22.

If we rescale variables, defining $\rho = r/R$ and $\mathbf{u} = \mathbf{v}_m / V_0$,

we find, to linear order in V_0,

$$\nabla^2\mathbf{u} - \nabla P' - \epsilon^2\mathbf{u} - \chi\,\hat{\mathbf{r}}\hat{\mathbf{r}}\cdot(\mathbf{u}-\hat{\mathbf{x}})\beta^2\frac{K_1^2(\beta\rho)}{K_0^2(\beta)} = 0 \quad (31)$$

$$\nabla\cdot\mathbf{u} = 0 \quad (32)$$

where the derivatives are now with respect to ρ, and P' is the unitless pressure. We now see that the velocity profile around the protein will depend on three dimensionless groups, ϵ, β, and χ, where $\epsilon = R/L_H$ and $\beta = R/\xi$ as above. The "drag ratio" $\chi \equiv \phi_b^2/\eta_m\Gamma$ is the ratio of the naive scale of the interaction drag $\zeta_I \sim \phi_b^2/\Gamma$ to the naive scale of the hydrodynamic drag, $\zeta_{\text{hydro}} \sim \eta_m$. By this, we mean that the naive model of Section I A (or that of Démery and Dean applied to Model A) predicts that the scale of the drag induced by the order-parameter interaction is ϕ_b^2/Γ, i.e. that the ratio of the order parameter drag to the hydrodynamic drag will scale as χ. However, increasing χ will also increase the effect that the order parameter has on the lipid flow near the protein, i.e. the last term in Eq. 31 becomes large if $\chi \gg 1$.

In order for the coupling between the protein and the order parameter field to alter the drag coefficient significantly, we must have $\chi \gg 1$. In this region of parameter space, the flow field $\mathbf{v}_m$ will necessarily be modified, and we will have to solve Eq. 31 numerically. Since the Stokes equations we use are two-dimensional, it turns out to be convenient to use the streamfunction representation for $\mathbf{u}$ [52]. We represent $\mathbf{u}(\rho,\theta) = \nabla\times[\psi(\rho,\theta)\hat{\mathbf{z}}]$, i.e.

$$u_\rho = \frac{1}{\rho}\frac{\partial}{\partial\theta}\psi(\rho,\theta) \quad (33)$$

$$u_\theta = -\frac{\partial}{\partial\rho}\psi(\rho,\theta) \quad (34)$$

which automatically satisfies the incompressibility requirement. We know by the linearity of the problem and the symmetry of $\mathbf{V}_p$, $\psi = Y(\rho)\sin\theta$. By taking the curl of Eq. 31, we find

$$\nabla^4\psi - \epsilon^2\nabla^2\psi + \chi\left(\frac{Y(\rho)}{\rho}-1\right)\frac{\beta^2}{\rho}\frac{K_1^2(\beta\rho)}{K_0^2(\beta)}\sin\theta = 0 \quad (35)$$

Or, explicitly working out the derivatives,

$$Y''''(\rho) + 2\frac{Y'''(\rho)}{\rho} - \left(\frac{3}{\rho^2}+\epsilon^2\right)Y''(\rho) + \left(\frac{3}{\rho^3}-\frac{\epsilon^2}{\rho}\right)Y'(\rho) - \left(\frac{3}{\rho^4}-\frac{\epsilon^2}{\rho^2}\right)Y(\rho) + \chi\left(\frac{Y(\rho)}{\rho}-1\right)\frac{\beta^2}{\rho}\frac{K_1^2(\beta\rho)}{K_0^2(\beta)} = 0 \quad (36)$$

This fourth-order ODE has boundary conditions set by the boundary conditions on $\mathbf{v}_m$, which are $v_m^r = V_0\cos\theta$ and $v_m^\theta = -V_0\sin\theta$ at $r = R$, and $v_m^r = 0$, $v_m^\theta = 0$ as $r\to\infty$; these transform to $Y(1) = Y'(1) = 1$ and $Y(\infty) = Y'(\infty) = 0$. This boundary value problem is relatively straightforward, though it does require us to resolve a large range of length scales; we must resolve the velocity field over the region $[1, 1+1/\beta]$ where $\phi_{(0)}$ is significantly different from zero, but the domain of the whole problem $[1,\rho_{\text{max}}]$ may be large, as we must have $\rho_{\text{max}} \gg 1/\epsilon$. We use MATLAB's boundary value solver bvp4c to determine $Y(\rho)$. We use an initial guess of $Y(\rho) = 1/\rho$ with a logarithmically-spaced initial mesh.

Once $Y(\rho)$ is determined, we need to calculate the total drag force, Eq. 24. We can do this in two major routes: 1) directly via Eq. 24, or 2) applying an identity derived from the reciprocal theorem [52–54]. Each route has separate advantages: if we use Eq. 24 directly, we do not need to determine $\phi_{(1)}$ explicitly, but if we use the reciprocal theorem identity, we need to determine $\phi_{(1)}$, but do not need to determine the full membrane stress tensor σ or the membrane pressure P. We determine the drag with both methods to ensure consistency (Appendix B). As a check on the accuracy of the solver and the drag calculation, for $\chi = 0$, we reproduce the Evans-Sackmann result Eq. 30 with a maximum relative error of 5×10^{-5} for ϵ from 10^{-5} to 10^5. These errors are for the direct method; the reciprocal theorem method uses the exact result Eq. 30, and does not provide an independent check if $\chi = 0$.

A. Implications for protein diffusion coefficients

The experiments of Gambin et al. measure the diffusion of proteins and protein complexes with radii ranging from $0.5-2$ nm [9], finding that $D\sim 1/R$ (i.e. $\zeta\sim R$) over this range. Experimentally measured membrane surface viscosities are of the order of $10^{-7}-10^{-5}$ poise cm [40, 55–58], corresponding to Saffman-Delbrück lengths ($L_{sd} = \eta_m/2\eta_f$) of roughly $0.1-10$ microns, much larger than the protein radius. The relevant hydrodynamic regime for describing proteins is thus $R \ll L_{sd}$. Many features of this limit are reproduced by our Brinkman equation model of Eq. 31. In particular, the Saffman-Delbrück drag and the Evans-Sackmann drag have the same scaling when $R \ll L_{sd}$ and $R \ll L_H$; for $\epsilon = R/L_H \ll 1$, the Evans-Sackmann drag has the form $\zeta_{\text{Evans-Sackmann}} \approx 4\pi\eta_m\left[\log(2/\epsilon)-\gamma_E\right]^{-1}$, in comparison with $\zeta_{sd} = 4\pi\eta_m\left[\log(2L_{sd}/R)-\gamma_E\right]^{-1}$ for $R\ll L_{sd}$. We wish to explore the question: can the interaction with the order parameter alone change the scaling of ζ to $\zeta\sim R$ in the region $\epsilon\ll 1$? Within our model of Section I A and that of DD, the answer is yes. However, we will find that including the advection of the lipids will qualitatively change the size of the effect, showing that (within our model), order parameter interactions are insufficient to explain the experimental data of [9].

In our model of Section I A, we found that the order-

parameter interaction led to $\zeta_{\text{tot}} \sim R$ in the limit of $R \gg \xi$ ($\beta \gg 1$) and $\chi \gg 1$; we will start by examining this region of parameter space. We can determine some of the characteristic features of the velocity profile $u_\rho(\rho,\theta) = \rho^{-1}Y(\rho)\cos\theta$ simply from Eq. 31. We see that the order-interaction term acts as an effective drag on the radial part of $\mathbf{u}$ relative to the protein's radial velocity, $\hat{\mathbf{r}}\cdot\hat{\mathbf{x}} = \cos\theta$. However, as $K_1(\beta\rho)$ will decay quickly for $\rho \gg 1/\beta$, this drag is only effective for a small region near the protein. If $\beta \gg 1$, we would expect that the order-interaction drag is negligible beyond a distance ρ^*, where $(\rho^* - 1) \sim \frac{1}{2\beta}\log\left[b\chi\beta^2\right]$ where b is an arbitrary constant. In our numerical results, we see that for strong protein-order parameter coupling, $\chi \gg 1$, the radial velocity near the protein is nearly constant for a significant distance (Fig. 7). This suggests the idea of an "effective radius" - that the order-induced drag essentially perfectly entrains the lipids within a characteristic distance of the protein, and the total drag should be simply $\zeta_{\text{Evans-Sackmann}}(\epsilon R_{\text{eff}}/R)$. Our estimate from above suggests that $(R_{\text{eff}}/R - 1) \sim \frac{1}{\beta}\left[\log\chi + \log b\beta^2\right]$ for $\beta \gg 1$. We find below that $(R_{\text{eff}}/R - 1) \sim \frac{1}{\beta}$ can also be a useful fitting form more generally; this is unsurprising, as it suggests that the effective radius is just the protein radius plus a distance on the order of the interface width ξ, i.e. $R_{\text{eff}} \approx R + c\,\xi$. However, we note that this is only a rough estimate, and in fact will break down for larger β or ϵ; this will be addressed further in Section II B.

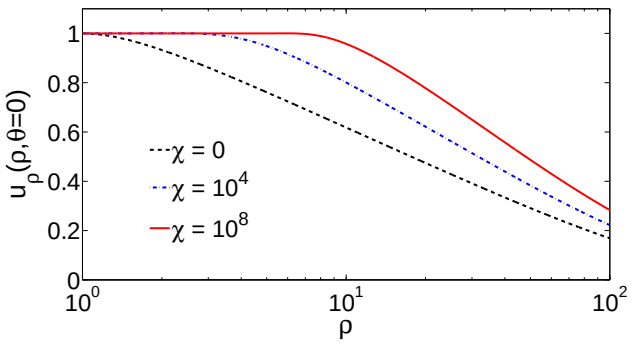

FIG. 7. (Color online). As $\chi = \phi_b^2/\Gamma\eta_m$ is increased, the lipids near the protein are increasingly correlated to the protein velocity, and the radial velocity profile u_ρ is constant over the "effective radius" of the protein, which increases weakly with increasing χ. For this figure, $\beta = 1$, $\epsilon = 10^{-2}$, and $\rho_{\text{max}} = 100/\epsilon$ (the entire domain is not shown in this figure).

At large χ, the total drag increases roughly linearly with $\log\chi$ (Fig. 8). By comparison, the theory of Section I A predicts that $\zeta_I/\eta_m \sim \chi$ (Eq. 10); entrainment significantly reduces the effect of the order parameter coupling. In fact, even increasing the coupling strength ϕ_b^2 by ten orders of magnitude produces a smaller than 10% change in the total drag. This weak dependence is consistent with the "local entrainment" argument given above: if we solve for the effective radius as defined by $\zeta_{\text{tot}}(\epsilon,\chi) = \zeta_{\text{Evans-Sackmann}}(\epsilon R_{\text{eff}}(\chi)/R)$, we find that it scales as $\log\chi$ for $\chi \gg 1$ (Fig. 8).

What is the effect of changing the size of the protein? For

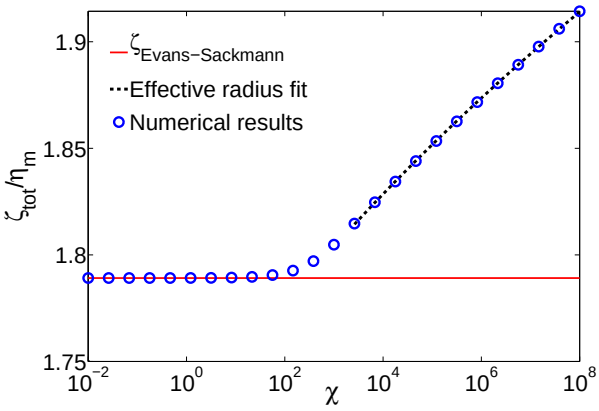

FIG. 8. (Color online). As $\chi = \phi_b^2/\Gamma\eta_m$ is increased, the total drag on the protein ζ_{tot} (Eq. 26) increases only slowly, roughly as $\log\chi$; this is very different from the theory of Section I A, which predicts that the drag should be linearly proportional to χ (Eq. 10). We can fit these results to an effective radius theory as suggested above, with $R_{\text{eff}}/R = 1 + c_1 + c_2\log\chi$ with $c_1 = -0.25$ and $c_2 = 0.045$. In this simulation, $\epsilon = 10^{-3}$, $\beta = 10$, and $\rho_{\text{max}} = 100/\epsilon$.

the model of Section I A, we found that the interaction drag ζ_I depended on the protein radius R only in the combination $\beta = R/\xi$. This will not be the case for the total drag in our hydrodynamic model. We can determine the total drag as we either vary the interface width (Fig. 9), or vary the protein radius (Fig. 10).

If we vary the correlation length ξ while holding the protein radius fixed, we find that smaller drag layers will lead to a smaller total drag on the particle (Fig. 9). This may seem unsurprising, but should be contrasted with the result in the absence of hydrodynamics, Eq. 10, where the interaction drag ζ_I is proportional to R/ξ, and thus smaller correlation lengths ξ lead to larger drags.

If we increase the protein radius, holding the interface width ξ and the hydrodynamic length L_H fixed, we see that the drag increases (Fig. 10), but not nearly as much as would be predicted by the model of Section I A. We find that as $R \gg \xi$, the effect of the order parameter coupling vanishes, and the total drag simply reduces to the hydrodynamic Evans-Sackmann drag, Eq. 30. This behavior, as well as that of Fig. 9, can be well-explained by a description of the protein locally entraining the nearby lipids, as mentioned earlier. The total drag coefficients can be simply fit to an "effective radius" model with $R_{\text{eff}} = R + c\xi$, with c a constant.

The effects of the order parameter interaction are most obvious for large correlation lengths. In Fig. 11, we show streamlines for flow past a protein with and without the order parameter coupling. In this example, the correlation length ξ is ten times the protein radius, making the "effective size" of the protein very large compared to the protein's physical size.

As we can see from Fig. 10 and Fig. 8, in the limit of $R \gg \xi$ and $R \ll L_H$, there is not a significant change in the total drag, and there is not a qualitative change in the scaling of the drag with radius R; instead, there is a weak dependence

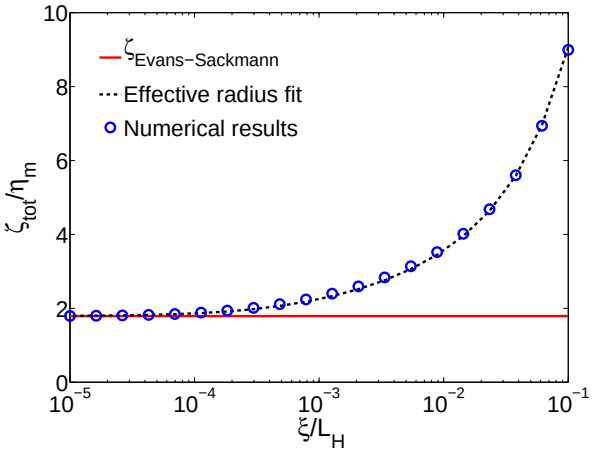

FIG. 9. (Color online). If we vary the correlation length of ϕ, ξ, while holding the radius R and the hydrodynamic length scale L_H fixed (corresponding to varying β while holding ϵ fixed), we see that smaller drag layers lead to smaller total drag $\zeta_{\rm tot}$ (Eq. 26) on the particle. This should be contrasted with the result in the absence of hydrodynamics, Eq. 10, in which thinner layers lead to larger gradients and thus larger drags. $\epsilon = 10^{-3}$ and $\chi = 10^6$ for the data in this figure. This is well fit to an effective radius of $R_{\rm eff}/R = 1 + c/\beta$ with $c = 3.22$.

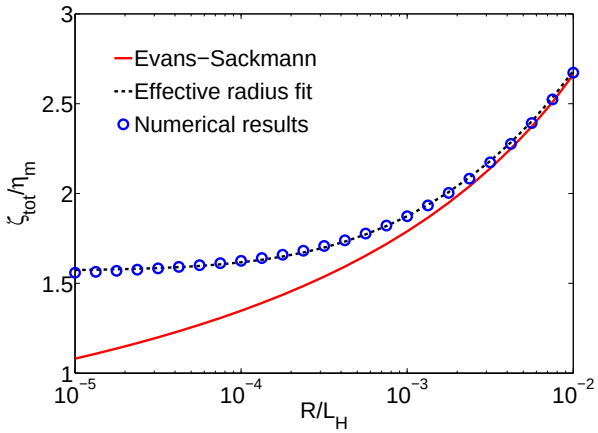

FIG. 10. (Color online). As the radius of the particle is increased, the additional drag from the order interaction becomes negligible and $\zeta_{\rm tot}$ (Eq. 26) approaches $\zeta_{\text{Evans-Sackmann}}$. In this figure, we vary R while keeping ξ and L_H fixed; we thus vary β and set $\epsilon = 10^{-4}\beta$, so that $\epsilon \ll 1$ for the entire range of ϵ studied (β ranges from 0.1 to 100). $\chi = 10^6$ for this figure. This is well fit to an effective radius of $R_{\rm eff}/R = 1 + c/\beta$ with $c = 3.73$.

that can be characterized in terms of an "effective radius" on the order of the protein size plus the interface size ξ. This behavior holds even in the limit of $\chi \gg 1$. This answers our central question: order parameter interactions, at least in this model, are not sufficient to cause the experimentally observed result [9] $\zeta_{\rm tot} \sim R$.

As far as we can tell, even as $\chi \gg 1$, we do not recover the model of Section I A, which predicts a linear increase in ζ_I with χ. This result is perhaps not surprising, as the models of Section I A and DD assume that lipid motion near the protein is completely uncorrelated to the protein (Fig. 5); this limit is not reached by increasing χ, which only tends to increase the entrainment of lipids near the protein (Fig. 7). The neglect of advection and hydrodynamics in the models of Section I A and that of [15, 16] are therefore not well justified.

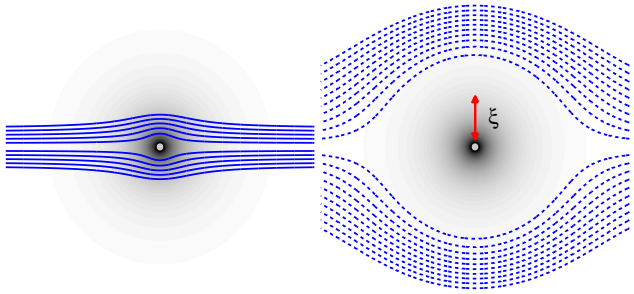

FIG. 11. (Color online). Streamlines for flow around a protein; streamlines are shown in the protein's rest frame. For the left panel, $\chi = 0$, i.e. there is no order-parameter coupling, and the flow reflects the physical size of the protein (central gray circle). In the right panel, there is strong order-parameter coupling, $\chi = 10^5$, with a thick interface, $\beta = 0.1$ ($\xi = 10R$), and show that flow is modified, resembling a particle with a much larger effective size. The order parameter profile $\phi_{(0)}(\rho)$ is also shown (grayscale shading). $\epsilon = 0.01$ for both cases.

B. Other interesting features of the model with advection

Though our primary interest in this model was to consider the limit relevant to the experiments on proteins of Gambin et al. [9], i.e. $R \ll L_H$ or $\epsilon \ll 1$, where the analogy to free membranes is best, our model (Eq. 36) also describes dynamics of larger objects in a supported membrane, $\epsilon > 1$. In this limit, the simple "effective size" picture is not as useful in determining the drag on a membrane-embedded object. We plot the total drag on the protein as a function of R/L_H for various values of ξ/L_H and χ in Fig. 12 and Fig. 13. We see that for R sufficiently large, the Evans-Sackmann result applies, as for the case of $\epsilon \ll 1$ above.

A striking exception to the "effective radius" idea also occurs for objects larger than the hydrodynamic correlation length L_H; we find that in this limit, the total drag depends *non-monotonically* on the interface width ξ, with an initial increase in drag followed by a decrease (Fig. 14). This runs counter to the intuition from above, where larger values of ξ lead to the lipids near the protein becoming increasingly entrained, and hence larger drags. However, in the limit of $\epsilon \gg 1$, increasing ξ does not necessarily increase the local entrainment of lipids. In fact, the range of entrainment decreases at large ξ. We show this explicitly in Fig. 15, where we plot the lipid velocity field near the protein as well as the distortion $\phi_{(0)}(\mathbf{r})$. Though this is initially unintuitive, an effect of this sort should not be altogether surprising. The drag

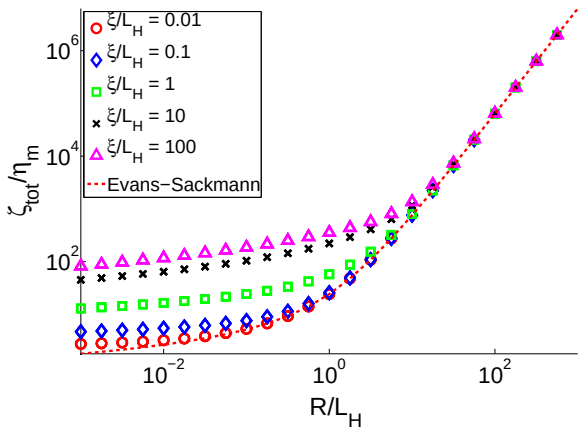

FIG. 12. (Color online). As the radius of the object increases, the additional drag from the order parameter interaction becomes negligible and the total drag $\zeta_{\rm tot}$ (Eq. 26) approaches the Evans-Sackmann result as $R \gg \xi, L_H$. Drag is shown as a function of $R/L_H = \epsilon$, with L_H and ξ held fixed. For this figure, $\chi = 10^3$. Only points with $\beta < 10^3$ are shown, for reasons of computation time.

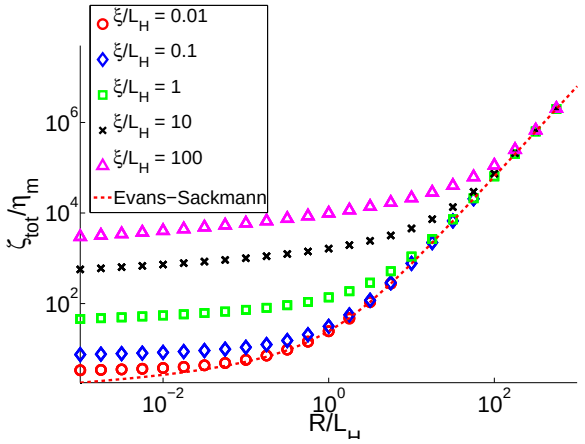

FIG. 13. (Color online). Increasing χ increases the total drag $\zeta_{\rm tot}$ on the protein, but does not change the qualitative features from that shown in Fig. 12. For this figure, $\chi = 10^5$, Only points with $\beta < 10^3$ are shown, for reasons of computation time.

III. DISCUSSION

We have presented a model that describes the drag on a protein due to its coupling to a non-conserved order parameter. Our model, though it uses the same underlying Model A dynamics as that of Démery and Dean [15, 16], couples the protein to the order parameter by imposing a boundary condition, and calculates the force via the stress tensor. This model shows that the interaction drag ζ_I scales linearly in the protein radius R if R is much larger than the order parameter correlation length, but has a much weaker, logarithmic, dependence on R for $R \ll \xi$. We attribute the difference between our result and that of Démery and Dean to the different handling of the protein-order parameter interaction, and show that by altering their method of assigning the linear coupling parameter h we can make the two methods consistent.

We also note that Démery and Dean have also calculated the drag force at large particle velocities $\mathbf{V}_p$, which we have not done. However, we suspect that our model of Section I A will also differ from the linear coupling model of Démery and Dean in terms of the nonlinear response. In [16], the distortion in ϕ caused by the object-field interaction vanishes as $1/\mathbf{V_p}$ at large velocities, but because of the boundary condition we force on the lipids due to the composition interaction takes the form of a force density proportional to the *gradient* of $\phi_{(0)}(\mathbf{r})$, $\mathbf{f}_\phi = -\Gamma^{-1}(\mathbf{v}_m - \mathbf{V}_p)\cdot\nabla\phi_{(0)}\nabla\phi_{(0)}$. As ξ increases, the order parameter field $\phi_{(0)}(\mathbf{r})$ becomes increasingly uniform, and the order-parameter drag is less effective at entraining local lipids (Fig. 15). However, this limit does not appear to have any immediate physical relevance, since it refers to distortions that are orders of magnitude larger than the protein they surround.

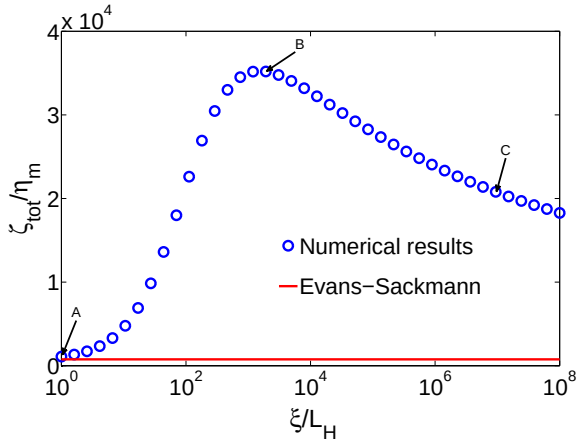

FIG. 14. (Color online). The total drag on the protein $\zeta_{\rm tot}$ (Eq. 26) can be non-monotonic in ξ, the size of the distortion of the ϕ field. The velocity field of the points marked A, B, and C are shown in Fig. 15. For this simulation, $\epsilon = 10$ and $\chi = 10^5$, and we set $\rho_{\rm max} = \max(100, 100/\beta)$ where $\beta = R/\xi$; this result is insensitive to increases in $\rho_{\rm max}$ and refinements of the mesh.

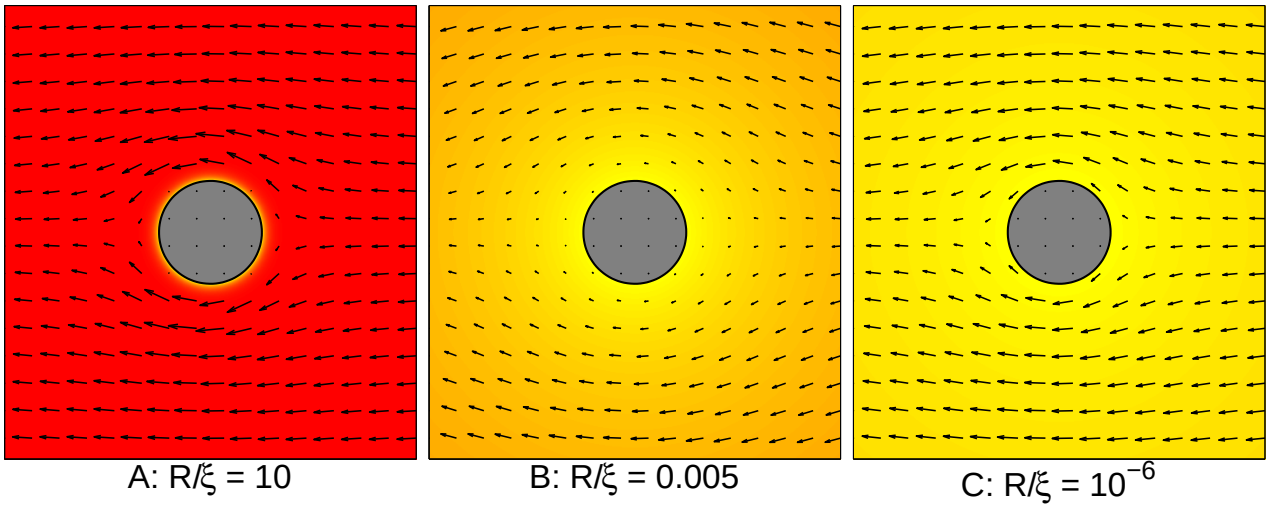

FIG. 15. (Color online). Lipid flow fields near the protein are superimposed over the distortion in the order parameter, $\phi_{(0)}(\mathbf{r})$, which is shown as a color map, ranging from light ($\phi = \phi_b$) to dark ($\phi = 0$). Velocities are plotted relative to the protein's velocity. In the leftmost image (A), the distortion is small, and does not strongly affect the velocities. In the center image (B), the distortion is large, extending far beyond the region shown, but still shows noticable gradients near the protein. In this limit, lipids are significantly correlated to the protein over a larger range than shown in A. In (C), the distortion is yet larger, and the gradient near the protein has decreased; lipids near the protein are not as entrained as in (B). The velocities have the same scale for (A),(B) and (C).

have chosen, there will always be a non-vanishing distortion in ϕ, though it may occur in a boundary layer near the protein, as in calculations of the nonlinear microrheological drag in colloidal model systems [53, 59].

Extending the model past dissipative dynamics to include advection of the order parameter (Section II), we discover that the hydrodynamics of Advected Model A significantly change the total drag on the protein, and hydrodynamics cannot be neglected in a consistent way. We find that once the fluid nature of the membrane is included, the protein-lipid complex acts like a protein with a larger effective radius, i.e. the lipids near the protein are almost completely entrained, at least for the most physically relevant parameters. This effective radius depends linearly on the order parameter correlation length ξ, but only weakly on the strength of the order parameter coupling. If the advection is included, the coupling to the order parameter does not change the drag scaling from logarithmic to linear in radius; there are quantitative, but not qualitative, deviations from the Evans-Sackmann result. Within Advected Model A, coupling to an order parameter as proposed by [14, 15] is not sufficient to explain the experimentally observed diffusion coefficient scaling $D = k_B T/\zeta_{\rm tot} \sim 1/R$ [9]. However, this may be a limitation of the the very simple model we have used; simulations of microrheology experiments in three-dimensional cholesteric liquid crystals have observed significant deviations from the Stokes drag, including a different dependence on particle size [60].

The work we have presented here is only an initial step toward more detailed understanding of the dynamics of protein-lipid coupling. However, because of the significant difference between the simplest possible Model A approach and a more detailed calculation that includes the in-plane membrane hydrodynamics, we argue that future calculations should, as we have done in Section II, address the hydrodynamic advection of the order parameter, as well as the effects of the inhomogeneity of the order parameter on lipid flows within the membrane. In particular, the dynamics of membrane tilt (see [29] and references within) may be able to be described using continuum theories for liquid crystal dynamics [26, 61]; to our knowledge, this approach has not yet been attempted, though relevant work has been done on the simulation of liquid-crystal elastomers with free boundaries [62]. An additional feature absent from our advective model is the potential dependence of membrane viscosity on the order parameter; if $\eta_m(\phi)$ is not constant, the drag coefficient of the protein may be modified [63].

Throughout this paper, we have neglected explicit fluctuations in the order parameter; this is effectively a zero-temperature assumption, i.e. that $\langle\phi^2\rangle \approx \langle\phi\rangle^2$. We note that for nonlinear couplings, there may be an additional "Casimir drag" caused by the suppression of thermal fluctuations [64]; this mechanism may also be relevant to the boundary condition coupling we use, as the stress tensor is nonlinear in ϕ. This effect will not appear in linear coupling models [15, 16]. The effects of this Casimir drag are also an interesting area of future study.

Coarse-grained molecular dynamics simulations [13, 17, 44, 65–68] may also be able to address the problem we have described here. However, we note that these models may not be quantitatively accurate in describing in-plane flow; mem-

brane surface viscosities measured in coarse-grained models [69] can be one to two orders of magnitude below their experimental values [40, 55–58].

To summarize, we have three central points. First, even with the same underlying dynamics, we get a different drag than that of Démery and Dean [15] if we handle the protein-field interaction in a different way. Second, we show that the effects of advection cannot be neglected in a straightforward way; there is a qualitative difference between models that allow lipids to flow in response to order inhomogeneities and those that do not. Finally, within the simple model we develop, the protein-membrane interaction alone cannot explain the experimentally observed scaling of protein diffusion coefficient with radius; for parameters that describe a protein, the effect of the order parameter interaction is only to give the protein an "effective size" set by the size of the membrane distortion.

ACKNOWLEDGMENTS

We thank David Dean, Paul Atzberger, and Phil Pincus for useful conversations and suggestions. This work was supported in part by the NSF (grant nos. CHE-0848809, CHE-032168) and the BSF (grant no. 2006285). B.A.C. acknowledges the support of the Fannie and John Hertz Foundation.

Appendix A: Explicit calculation of linear distortion in ϕ

We explicitly calculate the order parameter profile $\phi(\mathbf{r},t)$ to first order in the velocity V_0 for the model of Section I A. The equation of motion is (in steady state)

$$-\mathbf{V}_p\cdot\nabla\phi=-\frac{1}{\tau}\left(\phi-\xi^2\nabla^2\phi\right) \tag{A1}$$

We wish to solve to linear order, $\phi(\mathbf{r}) = \phi_{(0)} + V_0\phi_{(1)}$. We showed in the main body of the paper that $\phi_{(0)}(\mathbf{r}) = \phi_b\frac{K_0(r/\xi)}{K_0(R/\xi)}$. We then find that $\phi_{(1)}$ satisfies the equation

$$-\hat{\mathbf{x}}\cdot\nabla\phi_{(0)}=-\frac{1}{\tau}\left(\phi_{(1)}-\xi^2\nabla^2\phi_{(1)}\right) \tag{A2}$$

The solution to this equation will have the form $\phi_{(1)}(\mathbf{r},t) = f(r)\cos(\theta)$, with boundary conditions $f(r = R) = 0$, $f(r) \to 0$ as $r \to \infty$. $f(r)$ then satisfies a modified inhomogeneous Bessel equation,

$$\xi^2\left[f''+\frac{1}{r}f'-\frac{1}{r^2}f\right]-f=\frac{\tau}{\xi}\phi_b\frac{K_1(r/\xi)}{K_0(R/\xi)} \tag{A3}$$

This equation is solved by

$$f(r)=\frac{\phi_b\tau}{2\xi^2}\left[\frac{RK_1(r/\xi)}{K_1(R/\xi)}-\frac{rK_0(r/\xi)}{K_0(R/\xi)}\right] \tag{A4}$$

The total drag force, which is in the $\hat{\mathbf{x}}$ direction by symmetry, is (with Π from Eq. 6)

$$F=R\int_0^{2\pi}d\theta\;\Pi_{xj}(r=R,\theta)\hat{n}_j \tag{A5}$$

where $\hat{n}_j$ is the outward-pointing normal to the circle. Performing this calculation to first order in V_0, we find $\mathbf{F} = -\zeta_I\mathbf{V}_p$, with

$$\zeta_I=\pi R\mathcal{E}\,\xi^2 f'(R)\phi'_{(0)}(R) \tag{A6}$$

Plugging the known forms of $f(r)$ and $\phi_{(0)}$ into the equation yields Eq. 10.

Appendix B: Calculating hydrodynamic and interaction drag: direct and reciprocal methods

The total drag force on the protein is

$$\mathbf{F}_{\text{drag}}=\oint d\ell\,(\sigma+\Pi)\cdot\hat{\mathbf{n}} \tag{B1}$$

where the integral is around the boundary of the protein, $\hat{\mathbf{n}}$ the outward-pointing normal, Π is the stress tensor for the order parameter (Eq. 6) and σ the hydrodynamic stress tensor,

$$\sigma_{ij}=-P\delta_{ij}+\eta_m\left(\frac{\partial v_m^i}{\partial r_j}+\frac{\partial v_m^j}{\partial r_i}\right) \tag{B2}$$

where P is the membrane surface pressure and η_m the membrane surface viscosity. We note that there is also a potential intrinsic drag term between the protein and the substrate; see the main text and [41, 42] for details. We can calculate the total drag force in two main ways: 1) directly evaluating the integral around the protein's boundary, and 2) using the reciprocal theorem. In the direct evaluation method, we can determine the interaction drag either by explicitly finding the $O(\mathbf{V}_p)$ correction to the concentration field, $\phi_{(1)}$, or using the divergence theorem. The major advantage to the direct evaluation method is that the explicit solution of the advection-diffusion equation can be avoided, which reduces the number of boundary value problems to be solved.

1. Direct calculation using surface pressure

In order to calculate $\mathbf{F}^{\text{hydro}}_{\text{drag}} = \oint d\ell\,\sigma\cdot\hat{\mathbf{n}}$, we need to determine the surface pressure P. We can use the approach of [41]; we know by the symmetry of the problem that $P'(\rho,\theta) = h(\rho)\cos\theta$. We note $\hat{\theta}\cdot\nabla P' = -\frac{1}{\rho}h(\rho)\sin\theta$, and so we can extract $h(\rho)$ directly from the $\hat{\theta}$ component of Eq. 31,

$$h(\rho)=\frac{2}{\rho^2}Y(\rho)-\frac{2+\rho^2\epsilon^2}{\rho}Y'(\rho)+Y''(\rho)+\rho Y'''(\rho). \tag{B3}$$

This is exactly the result of [41], as there is no $\hat{\theta}$ component to the composition-induced drag at linear order. We can then perform the angular integral

$$\mathbf{F}^{\text{hydro}}_{\text{drag}}\cdot\hat{\mathbf{x}}=R\int_0^{2\pi}\left[\sigma_{\rho\rho}\cos\theta-\sigma_{\rho\theta}\sin\theta\right] \tag{B4}$$

yielding $\mathbf{F}_{\text{drag}}^{\text{hydro}} = -\zeta_{\text{hydro}}\mathbf{V}_p$, with

$$\zeta_{\text{hydro}} = \pi\eta_m\left(Y'''(1) - \epsilon^2\right). \tag{B5}$$

The interaction component of the drag can be computed either by explicitly determining the stress tensor Π to linear order in $\mathbf{V}_p$, or by using the advection-diffusion equation, as in Section I A.

a. *Determining linear correction $\phi_{(1)}$*

In order to determine the linear correction to the equilibrium order parameter field, we can solve the advection-diffusion equation Eq. 22 perturbatively in $\mathbf{V}_p$, similarly to the procedure used in Section A. To linear order in $\mathbf{V}_p$, with $\phi(\rho) = \phi_{(0)}(\rho) + \phi_b\tau g(\rho)\cos\theta$,

$$\left[g'' + \frac{1}{\rho}g' - \frac{1}{\rho^2}g\right] - \beta^2 g = \beta^3\left(1 - \frac{Y}{\rho}\right)\frac{K_1(\rho\beta)}{K_0(\beta)} \tag{B6}$$

The boundary conditions on this boundary-value problem are $g(1) = 0$ and $g(\rho) \to \infty$ as $\rho \to \infty$. This is straightforward to solve numerically once $Y(\rho)$ is found via the method in the main paper; we use bvp4c for this problem as well.

The function $g(\rho)$ can also be used with Eq. A6 to determine the interaction drag,

$$\zeta_I/\eta_m = -\chi\frac{\pi}{\beta}\frac{K_1(\beta)}{K_0(\beta)}g'(1). \tag{B7}$$

b. *Determining ζ_I without calculating $\phi_{(1)}$*

The interaction component of the drag can be computed without explicitly finding $\phi_{(1)}$. First, by the divergence theorem, we note

$$\mathbf{F}_{\text{drag}}^{\text{int}} = \oint d\ell\,\Pi\cdot\hat{\mathbf{n}} \tag{B8}$$

$$= -\int_{r\geq R} d^2r\,\nabla\cdot\Pi \tag{B9}$$

We can use Eq. 22 to determine $\frac{\delta H}{\delta\phi}\nabla\phi = -\frac{1}{\Gamma}(\mathbf{v}_m - \mathbf{V}_p)\cdot\nabla\phi\nabla\phi$. To linear order in V_0, this force only depends on the static profile $\phi_{(0)}$, giving us

$$\mathbf{F}_{\text{drag}}^{\text{int}} = \frac{1}{\Gamma}\int_{r\geq R} d^2r\,(\mathbf{v}_m - \mathbf{V}_p)\cdot\nabla\phi_{(0)}\nabla\phi_{(0)} \tag{B10}$$

$$= \pi\frac{\mathbf{V}_p}{\Gamma}\int_1^\infty d\rho\,\rho\left(\frac{Y(\rho)}{\rho} - 1\right)\frac{K_1^2(\rho\beta)}{K_0^2(\beta)} \tag{B11}$$

i.e.

$$\zeta_I/\eta_m = \pi\chi\int_1^\infty d\rho\,\rho\left(1 - \frac{Y(\rho)}{\rho}\right)\frac{K_1^2(\rho\beta)}{K_0^2(\beta)} \tag{B12}$$

2. Reciprocal theorem method

The integral $\oint d\ell\,(\sigma + \Pi)\cdot\hat{\mathbf{n}}$ may also be evaluated simply by using an identity derived from the reciprocal theorem [52] of low-Reynolds number fluid mechanics (see [53, 54] and references within). This trick lets us determine the total drag force on an object in a fluid flow $\mathbf{v}$ in terms of a simpler "reference" flow $\tilde{\mathbf{v}}$ in the same geometry.

Suppose that $\mathbf{v}$ and $\tilde{\mathbf{v}}$ are two vector fields defined over the volume V outside a surface S, and $\nabla\cdot\mathbf{v} = \nabla\cdot\tilde{\mathbf{v}} = 0$. Then let σ and $\tilde{\sigma}$ be the hydrodynamic stress tensors corresponding to $\mathbf{v}$ and $\tilde{\mathbf{v}}$, i.e. $\sigma_{ij} = -P(\mathbf{r})\delta_{ij} + \eta\left[\partial_i v_j + \partial_j v_i\right]$, $\tilde{\sigma}_{ij} = -\tilde{P}(\mathbf{r})\delta_{ij} + \eta\left[\partial_i\tilde{v}_j + \partial_j\tilde{v}_i\right]$. Then

$$\int dS\hat{\mathbf{n}}\cdot\left[\mathbf{v}\cdot\tilde{\sigma} - \tilde{\mathbf{v}}\cdot\sigma\right] = \int dV\left[\tilde{\mathbf{v}}\cdot(\nabla\cdot\sigma) - \mathbf{v}\cdot(\nabla\cdot\tilde{\sigma})\right] \tag{B13}$$

where the normals $\hat{\mathbf{n}}$ point out from the surface. This result can be derived in any dimension using the divergence theorem.

We can use this to reformulate the integral $\mathbf{F}_{\text{drag}} = \oint d\ell\,(\sigma+\Pi)\cdot\hat{\mathbf{n}}$; in this case, the surface S is just the perimeter of the protein, $r = R$, and the volume V is the region outside of the protein, $r > R$. We let $\mathbf{v}$ be a solution to the drag problem of the membrane Stokes equation including the composition force $\nabla\cdot\Pi$, i.e. $\mathbf{v}$ obeys Eq. 27 with the boundary conditions $\mathbf{v} = \mathbf{V}_p$ at $r = R$, and $\mathbf{v} \to 0$ as $r \to \infty$. We then choose $\tilde{\mathbf{v}}$ to be the Evans-Sackmann solution [41], i.e. the solution of Eq. 27 with $\nabla\cdot\Pi = 0$ with the boundary conditions $\tilde{\mathbf{v}} = \tilde{\mathbf{V}}_p$ at $r = R$, and $\tilde{\mathbf{v}} \to 0$ as $r \to \infty$.

As the membrane Stokes equation (Eq. 27) can be written as $\nabla\cdot\sigma + \nabla\cdot\Pi - \frac{\eta_f}{H}\mathbf{v}_m = 0$, we find

$$\nabla\cdot\sigma = -\nabla\cdot\Pi + \frac{\eta_f}{H}\mathbf{v} \tag{B14}$$

$$\nabla\cdot\tilde{\sigma} = \frac{\eta_f}{H}\tilde{\mathbf{v}} \tag{B15}$$

Using these results, and noting that on the boundary of the protein, $\mathbf{v} = \mathbf{V}_p$ and $\tilde{\mathbf{v}} = \tilde{\mathbf{V}}_p$, we can simplify the reciprocal theorem relation (Eq. B13), finding

$$\tilde{\mathbf{V}}_p\cdot\oint d\ell\hat{\mathbf{n}}\cdot\sigma - \int_{r\geq R} d^2r\tilde{\mathbf{v}}\cdot(\nabla\cdot\Pi) = -\mathbf{V}_p\cdot\oint d\ell\hat{\mathbf{n}}\cdot\tilde{\sigma} \tag{B16}$$

Noting $\tilde{\mathbf{v}}\cdot(\nabla\cdot\Pi) = \nabla\cdot(\tilde{\mathbf{v}}\cdot\Pi) - \nabla\tilde{\mathbf{v}} : \Pi$ (where $\nabla\tilde{\mathbf{v}} : \Pi = (\partial_i\tilde{v}_j)\Pi_{ij}$) and applying the divergence theorem,

$$\tilde{\mathbf{V}}_p\cdot\oint d\ell\hat{\mathbf{n}}\cdot[\sigma + \Pi] = -\mathbf{V}_p\cdot\oint d\ell\hat{\mathbf{n}}\cdot\tilde{\sigma} - \int_{r\geq R} d^2r\nabla\tilde{\mathbf{v}} : \Pi. \tag{B17}$$

or

$$\tilde{\mathbf{V}}_p\cdot\mathbf{F}_{\text{drag}} = -\zeta_{\text{Evans-Sackmann}}\tilde{\mathbf{V}}_p\cdot\mathbf{V}_p - \int_{r\geq R} d^2r\nabla\tilde{\mathbf{v}} : \Pi \tag{B18}$$

We note that $\zeta_{\text{Evans-Sackmann}}$ as used in this equation does not include the "intrinsic drag" term addressed above, and so is smaller than Eq. 30 by $\pi\eta_m\epsilon^2$. This equation writes the drag on the protein only in terms of the reference flow and the

composition stress tensor Π. To determine Π to leading order in $\mathbf{V}_p$, we will have to solve the advection-diffusion equation numerically. Once this is done, and we know $\phi_{(1)}(\rho,t) = \phi_b \tau g(\rho)\cos(\theta)$, Eq. B18 yields $\mathbf{F}_{\text{drag}} = -\zeta_{\text{tot}}\mathbf{V}_p$, with

$$\zeta_{\text{tot}}/\eta_m = \frac{1}{\eta_m}\zeta_{\text{Evans-Sackmann}} + \chi\int_1^\infty d\rho\,\frac{\pi}{\beta}\frac{K_1(\rho\beta)}{K_0(\beta)}\frac{1}{\rho^2}\left\{[g(\rho)-2\rho g'(\rho)]\,[Y(\rho)-\rho Y'(\rho)] + \rho^2 g(\rho)Y''(\rho)\right\} \tag{B19}$$

3. Comparison of different calculation methods

We have found that as long as we solve the Stokes equations on a sufficiently large domain that the boundary conditions $Y(\rho_{\text{max}}) = Y'(\rho_{\text{max}}) = 0$ can reasonably be applied, the different solution techniques agree well (Fig. 16).

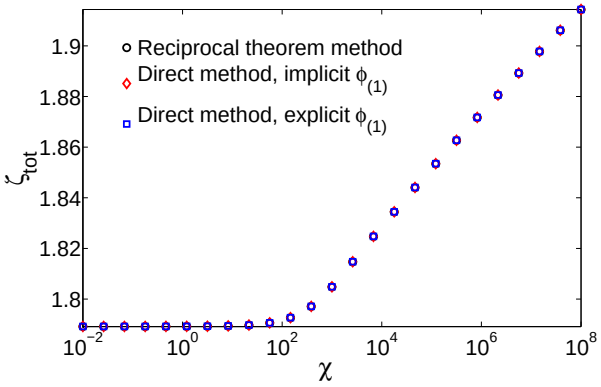

FIG. 16. (Color online). Calculation of ζ_{tot} does not depend strongly on the numerical method used. The maximum relative difference between these methods is 4×10^{-5}. Parameters in this calculation are the same as Fig. 8.

[1] R. B. Gennis, Biomembranes: Molecular Structure and Function (Springer-Verlag, Berlin, 1989).
[2] M. O. Jensen and O. G. Mouritsen, Biochim. Biophys. Acta. **1666**, 205 (2004).
[3] A. Lee, Biochim. Biophys. Acta. **1612**, 1 (2003).
[4] P. G. Saffman and M. Delbrück, Proc. Nat. Acad. Sci. USA **72**, 3111 (1975).
[5] B. D. Hughes, B. A. Pailthorpe, and L. R. White, J. Fluid Mech. **110**, 349 (1981).
[6] P. Almeida and W. Vaz, in Handbook of Biological Physics, edited by R. Lipowsky and E. Sackmann (Elsevier Science B.V., 1995).
[7] A. Pralle, P. Keller, E.-L. Florin, K. Simons, and J. Hörber, J. Cell Biol. **148**, 997 (2000).
[8] N. Tsapis, F. Reiss-Hunsson, R. Ober, M. Genest, R. Hodges, and W. Urbach, Biophys. J. **81**, 1613 (2001).
[9] Y. Gambin, R. Lopez-Esparza, M. Reffay, E. Sierecki, N. S. Gov, M.Genest, R. S. Hodes, and W. Urbach, Proc. Nat. Acad. Sci. USA **103**, 2098 (2006).
[10] Y. Gambin, M. Reffay, E. Sierecki, F. Hombl, R. S. Hodges, N. S. Gov, N. Taulier, and W. Urbach, J. Phys. Chem. B **114**, 3559 (2010).
[11] J. Kriegsmann, I. Gregor, I. Von Der Hocht, J. Klare, M. Engelhard, J. Enderlein, and J. Fitter, Chembiochem **10**, 1823 (2009).
[12] S. Ramadurai, A. Holt, V. Krasnikov, G. Van Den Bogaart, J. A. Killian, and B. Poolman, J. Am. Chem. Soc. **131**, 12650 (2009).
[13] S. Ramadurai, A. Holt, L. V. Schäfer, V. V. Krasnikov, D. T. S. Rijkers, S. J. Marrink, J. A. Killian, and B. Poolman, Biophysical Journal **99**, 1447 (2010).
[14] A. Naji, A. J. Levine, and P. Pincus, Biophys. J. **93**, L49 (2007).
[15] V. Démery and D. S. Dean, Phys. Rev. Lett. **104**, 080601 (2010).
[16] V. Démery and D. S. Dean, Europhys. J. E. **32**, 377 (2010).
[17] G. Guigas and M. Weiss, Biophys. J. **95**, L25 (2008).
[18] A. Naji, P. J. Atzberger, and F. L. H. Brown, Phys. Rev. Lett. **102**, 138102 (2009).
[19] E. Reister-Gottfried, S.M. Leitenberger, and U. Seifert, Phys. Rev. E. **75**, 011908 (2007).
[20] P. C. Hohenberg and B. I. Halperin, Rev. Mod. Phys. **49**, 435 (1977).
[21] P. M. Chaikin and T. C. Lubensky, Principles of Condensed Matter Physics (Cambridge University Press, 2000).
[22] T. M. Squires and T. G. Mason, Annu. Rev. Fluid. Mech. **42**, 413 (2010).
[23] T. Murtola, T. Róg, E. Falck, M. Karttunen, and I. Vattulainen, Phys. Rev. Lett. **97**, 238102 (2006).
[24] T. Yamamoto and S. A. Safran, Soft Matter **7**, 7021 (2011).
[25] T. Yamamoto, R. Brewster, and S. Safran, Europhys. Lett. **91**, 28002 (2010).
[26] A. N. Beris and B. J. Edwards, Thermodynamics of flowing systems with internal microstructure (Oxford University Press, New York, 1994).
[27] H. Stark and D. Ventzki, Phys. Rev. E. **64**, 031711 (2001).
[28] M. E. Cates, O. Henrich, D. Marenduzzo, and K. Stratford, Soft Matter **5**, 3791 (2009).
[29] M. C. Watson, E. S. Penev, P. M. Welch, and F. L. Brown, J. Chem. Phys **135**, 244701 (2011).
[30] M. Nagao, S. Chawang, and T. Hawa, Soft Matter **7**, 6598 (2011).
[31] E. Lindahl and O. Edholm, Biophys. J. **79**, 426 (2000).
[32] J. Wohlert and O. Edholm, J. Chem. Phys. **125**, 204703 (2006).
[33] N. Shimokawa, S. Komura, and D. Andelman, Eur. Phys. J. E. **26**, 197 (2008).
[34] P. de Gennes, Phys. Lett. A **30**, 454 (1969).
[35] M. Doi and S. F. Edwards, The Theory of Polymer Dynamics (Clarendon Press, 1999).
[36] Of course, this is really a perturbation series in the Peclet number $\mathrm{Pe} = V_0\tau/R$, where V_0 is the characteristic velocity scale, R the protein radius, and $\tau = 1/\Gamma\mathcal{E}$ is the characteristic relaxation time of the ϕ field.
[37] A.-F. Bitbol and J.-B. Fournier, Phys. Rev. E **83**, 061107 (2011).
[38] A. Onuki, J. Phys. Cond. Matt. **9**, 6119 (1997).
[39] B. J. Reynwar and M. Deserno, Biointerphases **3**, FA117 (2008).
[40] E. P. Petrov and P. Schwille, Biophys. J. **94**, L41 (2008).
[41] E. Evans and E. Sackmann, J. Fluid Mech. **194**, 553 (1988).
[42] H. A. Stone and A. Ajdari, J. Fluid Mech. **369**, 151 (1998).
[43] F. L. Brown, Quarterly Reviews of Biophysics **44**, 391 (2011).
[44] P. S. Niemalä, M. S. Miettinen, L. Monticelli, H. Hammaren, P. Bjelkmar, T. Murtola, E. Lindahl, and I. Vattulainen, J. Am. Chem. Soc. **132**, 7574 (2010).
[45] M. Chilcott and J. Rallison, J. Non-Newton. Fluid Mech. **29**, 381 (1988).
[46] D. K. Lubensky and R. E. Goldstein, Phys. Fluids **8**, 843 (1996).
[47] A. J. Levine and F.C. MacKintosh, Phys. Rev. E **66**, 061606 (2002).
[48] B. A. Camley and F. L. H. Brown, Phys. Rev. Lett. **105**, 148102 (2010).
[49] N. Oppenheimer and H. Diamant, Phys. Rev. E. **82**, 041912 (2010).
[50] K. Seki and S. Komura, Phys. Rev. E. **47**, 2377 (1993).
[51] S. Ramachandran, S. Komura, M. Imai, and K. Seki, Eur. Phys. J. E. **31**, 303 (2010).
[52] L. G. Leal, Advanced Transport Phenomena (Cambridge University Press, New York, 2007).
[53] R. J. DePuit, A. S. Khair, and T. M. Squires, Phys. Fluids **23**, 063102 (2011).
[54] B. Ho and L. Leal, J. Fluid Mech. **65**, 365 (1974).
[55] R. Dimova et al., Eur. Phys. J. B **12**, 589 (1999).
[56] R. Dimova, B. Pouligny, and C. Dietrich, Biophys. J. **79**, 340 (2000).
[57] P. Cicuta, S. L. Keller, and S. L. Veatch, J. Phys. Chem. B **111**, 3328 (2007).
[58] B. A. Camley, C. Esposito, T. Baumgart, and F. L. H. Brown, Biophys. J. **99**, L44 (2010).
[59] T. M. Squires and J. F. Brady, Phys. Fluids **17**, 073101 (2005).
[60] J. S. Lintuvuori, K. Stratford, M. E. Cates, and D. Marenduzzo, Phys. Rev. Lett. **105**, 178302 (2010).
[61] P. de Gennes and J. Prost, The Physics of Liquid Crystals (Oxford University Press, New York, 1995).
[62] W. Zhu, M. Shelley, and P. Palffy-Muhoray, Phys. Rev. E. **83**, 051703 (2011).
[63] A. J. Levine and T.C. Lubensky, Phys. Rev. E **65**, 011501 (2001).
[64] V. Démery and D. S. Dean, Phys. Rev. E **84**, 010103R (2011).
[65] M. Venturoli, B. Smit, and M. M. Sperotto, Biophys. J. **88**, 1778 (2005).
[66] G. Guigas and M. Weiss, Biophys. J. **91**, 2393 (2006).
[67] E. Lindahl and M. S. Sansom, Curr. Op. Struct. Bio. **18**, 425 (2008).

[68] L. Monticelli, S. K. Kandasamy, X. Periole, R. G. Larson, D. P. Tieleman, and S.-J. Marrink, J. Chem. Theory and Comput. **4**, 819 (2008).
[69] W. den Otter and S. Shkulipa, Biophys. J. **93**, 423 (2007).